Rapid Communications

Electronic spectral function in the fractionalized pair density wave scenario

M. Grandadam,[1] D. Chakraborty,[1,*] X. Montiel,[2] and C. Pépin[1]

[1]*Institut de Physique Théorique, Université Paris-Saclay, CEA, CNRS, F-91191 Gif-sur-Yvette, France*

[2]*Department of Materials Science & Metallurgy, University of Cambridge, 27 Charles Babbage Road, Cambridge CB3 0FS, United Kingdom*

(Received 4 March 2020; revised 11 June 2020; accepted 12 June 2020; published 9 September 2020)

Studies of the electronic spectral function in cuprates by angle-resolved photoemission spectroscopy (ARPES) reveal unusual features in the pseudogap phase that persist in the superconducting phase. Here we address these observations based on the recently proposed idea that the pseudogap is due to the fractionalization of modulated particle-particle pairs (a pair density wave) into uniform particle-particle and modulated particle-hole pairs. The constraint that appears between these two types of pairs can be seen has an amplitude for the pseudogap energy scale. This constraint directly modifies the electronic spectral function in the pseudogap phase. We derive a self-consistent equation for the pseudogap amplitude and show that it leads to the formation of Fermi arcs. The band dispersion obtained in the antinodal region is in good agreement with experimental ARPES observations in $Pb_{0.55}Bi_{1.5}Sr_{1.6}La_{0.4}CuO_{6+\delta}$ (Bi2201) and present a back-bending that goes to the Fermi level as we go away from the antinodal region. We also discuss the temperature dependence of the ARPES spectrum in the pseudogap and in the superconducting state.

DOI: 10.1103/PhysRevB.102.121104

Despite their discovery more than 30 years ago, there is still no consensus on the nature of the pseudogap (PG) phase of cuprate superconductors. This mysterious phase that emerges upon doping the parent Mott insulator shows many unusual features, the main one being a loss of density of states [1,2] as the temperature is decreased below a temperature T^*. In this study, we discuss a recent proposal where the opening of the pseudogap is attributed to the fractionalization of a pair density wave (PDW) [3]. Within this framework, we discuss the complex phenomenology of angle-resolved photoemission spectroscopy (ARPES) in nearly optimally doped $Pb_{0.55}Bi_{1.5}Sr_{1.6}La_{0.4}CuO_{6+\delta}$ (Bi2201). ARPES has proven to be one of the key probes in studying cuprates. It has notably been able to connect the loss of density of states in the pseudogap to the Fermi surface being gapped out in the antinodal region (ANR) for momenta close to $(0, \pm\pi)$, $(\pm\pi, 0)$, while other parts of the Fermi surface remain unchanged and form "Fermi arcs." (For a review of the pseudogap phenomenology, see, e.g., [4,5].)

Most remarkably one observes, in the ANR, a back-bending at a momentum k_G larger than the normal state Fermi momentum k_F, which suggested the presence of a modulation vector intimately linked with the opening of the pseudogap [6]. Moreover, as noticed in Ref. [7], the gap continuously closes from "below" when moving towards the Fermi arcs, which is interpreted as revealing the presence of particle-particle pairs in the PG. Lastly, one observes that the bottom of the band at $k = (0, \pi)$ drops when decreasing the temperature and a new lightly dispersive "flat" band is seen in superconducting phase. Few other scenarios have been proposed to explain this specific gaping mechanism such as a quantum disorder PDW [8], a coexistence of charge density wave (CDW) and PDW [9] or a resonant excitonic state (RES) [10]. In comparison to previous works, our study is based on a simple intuition, and accounts for all the experimental features with very few adjusting parameters.

This Rapid Communication is organized as follows. We start with a self-consistent equation for the pseudogap amplitude by treating a model of itinerant electrons interacting through antiferromagnetic exchange and residual density-density interaction at the mean-field level. The pseudogap can be seen as a superposition of superconductivity (SC) and CDW orders resulting in a composite order which has a nonzero amplitude in the ANR leading to the formation of Fermi arcs. The electronic spectral function in the ANR shows all the specific features mentioned previously, namely, we obtain a back-bending of the electronic dispersion, a flatband and the gap closing from below when going closer to the center of the Brillouin zone. The effects of temperature on the spectral function close to $k = (\pi, 0)$ and on the spectral weight of the flatband are also discussed based on phenomenological arguments.

The fractionalization of a PDW order is written in a way resembling the fractionalization of the electron introduced in strong-coupling theories [11–13]. The assumption is that, at a certain energy scale E^*, the system wants to form a PDW, which is depicted locally as an η mode [3,14]

$$\hat{\eta} = [\hat{\Delta}_{ij}, \hat{\chi}_{ij}^{\dagger}], \quad \hat{\eta}^{\dagger} = [\hat{\chi}_{ij}, \hat{\Delta}_{ij}^{\dagger}], \tag{1}$$

where $\hat{\Delta}_{ij} = \hat{d}_{ij} \sum_{\sigma} \sigma c_{i,\sigma} c_{j,-\sigma}$ and $\hat{\chi}_{ij} = \hat{d}_{ij} \sum_{\sigma} c_{i,\sigma}^{\dagger} c_{j,\sigma} e^{i\mathbf{Q}\cdot(\mathbf{r_i}+\mathbf{r_j})/2}$ are, respectively, the SC and CDW operators, $\hat{d}_{ij}$ being a structure factor which can assume d-wave symmetry and $\boldsymbol{Q}$ is the modulation wave vector of the PDW. The η

*Present address: Department of Physics and Astronomy, Uppsala University, Box 516, S-751 20 Uppsala, Sweden.

operators are invariant with the following gauge structure:

$$\hat{\Delta}_{ij} \to e^{i\theta}\hat{\Delta}_{ij}, \quad \hat{\chi}_{ij} \to e^{i\theta}\hat{\chi}_{ij}. \tag{2}$$

Then, the effective field theory for the fluctuating PDW is a rotor model [15], in which the fluctuation of the U(1) gauge field produces a constraint between the two fields:

$$|\hat{\Delta}_{ij}|^2 + |\hat{\chi}_{ij}|^2 \equiv |\Psi_{ij}|^2 = \text{const}, \tag{3}$$

where $\Psi_{ij} = (\hat{\Delta}_{ij}, \hat{\chi}_{ij})^t$. The energy scale associated to Eq. (3) is typically the scale at which the fractionalization occurs. In our ansatz, it corresponds to the PG scale which we denote $|\Psi_{ij}| = E^*$ [3,15] in analogy with the pseudogap temperature T^*.

The goal of this Rapid Communication is to test the validity of this unusual proposal by studying the fine structure of the spectral weight against the observations made by ARPES in Bi2201. For this we start with electrons hopping on a square lattice interacting via an effective antiferromagnetic coupling J_{ij}, which comes, for example, from the Anderson superexchange mechanism, and a small off-site residual Coulomb interaction term V_{ij}:

$$H = \sum_{i,j,\sigma} t_{ij}(c^\dagger_{i\sigma}c_{j\sigma} + \text{H.c.}) + J_{ij}\,\boldsymbol{S}_i \cdot \boldsymbol{S}_j + V_{ij}\,n_i n_j, \tag{4}$$

where $c^\dagger_{i\sigma}$ is the creation operator for an electron with spin σ on a site i, $\boldsymbol{S_i} = c^\dagger_{i\alpha}\boldsymbol{\sigma}_{\alpha\beta}c_{i\beta}$ is the spin operator with $\boldsymbol{\sigma}$ the vector of Pauli matrices, and t_{ij} describe hopping between different sites and are taken from a fit to ARPES data [6,10,15]. Both interactions are restricted to nearest neighbors and we take V to be smaller than J, which will be our main energy scale.

We treat this model in momentum space and start by decoupling the interaction with the individual fields forming the doublet. Here these fields are a pairing field Δ_k and four density modulation fields χ_k with uniaxial modulation vectors $Q = \pm Q_x; \pm Q_y = (\pm Q_0, 0); (0, \pm Q_0)$ shown in Fig. 1(a). The effective action for the doublet $\Psi^\dagger_k = (\Delta^*_k,\ \chi_k{}^*)$ representing our pseudogap is then given by [15]

$$\mathcal{S}_{eff} = \int d\tau \sum_{Q,k,q} \frac{{\Psi_k}^\dagger \Psi_{k+q}}{\tilde{J}(q)} - \text{Tr}\ln[G^{-1}(i\omega, k)], \tag{5}$$

$$G^{-1}(i\omega, k) = i\omega - \xi_k - \sum_{Q=\pm Q_x, \pm Q_y} \frac{|\Psi_k|^2}{2}\tilde{G}(i\omega, k), \tag{6}$$

where ξ_k is the noninteracting electronic dispersion, $\tilde{G}(i\omega, k) = (i\omega - \xi_{k+Q})^{-1} + (i\omega + \xi_k)^{-1}$, and $1/\tilde{J} = 3J/(9J^2 - V^2)$. The electronic Green's function in Eq. (6) will thus be modified if $|\Psi_k|$ acquires a nonzero value even if both the composing fields are fluctuating and have a vanishing expectation value.

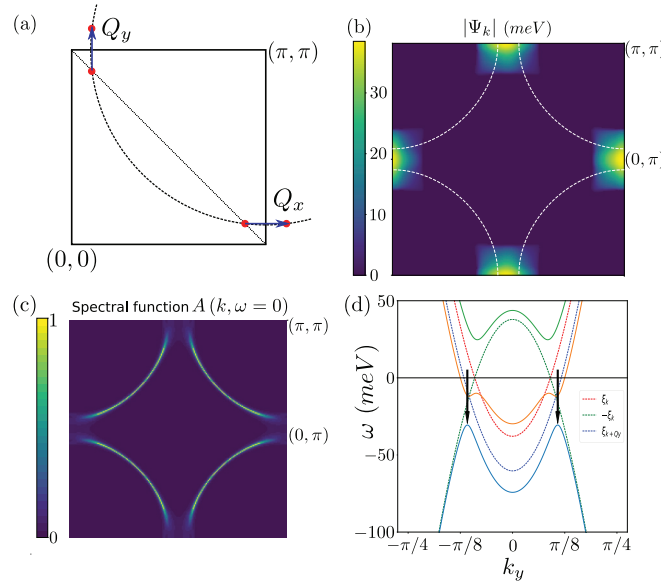

FIG. 1. (a) Schematic representation of the Brillouin zone for cuprates with the modulation wave vector used in this work. (b) Solution of the gap equation for the pseudogap amplitude Eq. (7). Colored regions show nonzero solutions for $|\Psi_k|$. We used an axial modulation wave vector Q_x relating hot spots shown in panel (a) and $J = 300$ meV, $V = J/10$, and $q_{AF} = 0.15$ r.l.u. The white line indicates the noninteracting Fermi surface. (c) Electronic spectral function $A(k, \omega = 0)$ obtained from Eq. (6) for $|\Psi_k|$ given by Eq. (7). We see the formation of Fermi arcs as the ANR gets gapped out. We used a broadening factor $\eta = 5$ meV for numerical purposes. (d) Band structure obtained by the Green's function in Eq. (6) for $k_x = \pi$ and a constant $|\Psi_k| = 30$ meV. The dotted lines indicate the noninteracting dispersion ξ_k (red), the hole band $-\xi_k$ (green), and the band from the modulating order ξ_{k+Q_x} (blue). The black arrows point to the back-bending mentioned in the main text.

Minimizing $\mathcal{S}_{eff}$ in Eq. (5) with respect to the doublet Ψ_k gives the mean-field gap equation for the doublet amplitude. We will consider the different modulation wave vectors to be decoupled and use the fact that $\tilde{J}_{\boldsymbol{q}}$ is peaked around $\boldsymbol{q} = (\pi, \pi)$ to restrict the momentum summation to a range q_{AF} around the antiferromagnetic wave vector. The parameter q_{AF} is physically associated with the short-range nature of the antiferromagnetic fluctuations [16] mediating the interaction. Assuming that $|\Psi_k|$ is constant over a range q_{AF}, the self-consistent equation is of the BCS form:

$$|\Psi_k| = -\frac{T}{N}\sum_{i\omega_n, \tilde{q}} \tilde{J}\left(i\omega_n + \frac{\Delta\xi_{k+\tilde{q}}}{2}\right) \frac{|\Psi_{k+\pi}|}{\left[(i\omega_n)^2 - \xi^2_{k+\tilde{q}}\right](i\omega_n - \xi_{k+Q+\tilde{q}}) - \left(i\omega_n + \frac{\Delta\xi_{k+\tilde{q}}}{2}\right)|\Psi_{k+\pi}|^2}, \tag{7}$$

where $\tilde{q}$ range between $\pi - q_{AF}/2$ and $\pi + q_{AF}/2$ and $\Delta\xi_{k+q} = \xi_{k+q} - \xi_{k+Q+q}$. Ignoring frequency dependence of $|\Psi_k|$ we can perform the Matsubara summation analytically. This leads to two coupled equations between $|\Psi_k|$ and $|\Psi_{k+\boldsymbol{\pi}}|$ which we can solve self-consistently.

Results of this self-consistent equation are shown in Fig. 1(b) for a modulation wave vector linking hot spots along

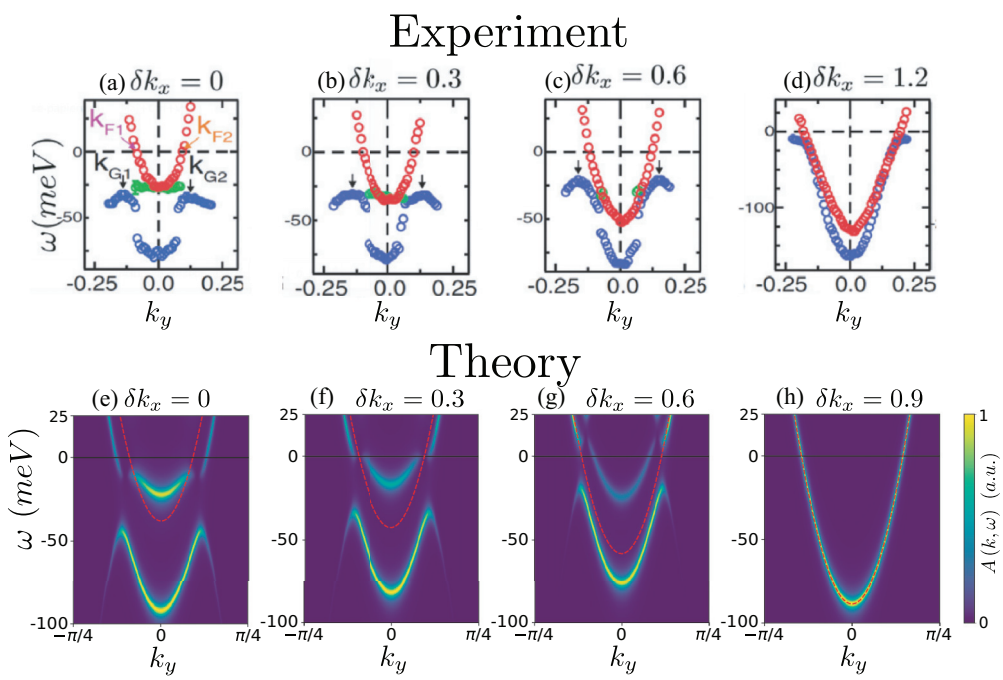

FIG. 2. (a)–(d) Experimental dispersion obtained by ARPES [6] for $T > T^*$ (red dots) and $T < T_c$ (blue and green dots) for different cuts at fixed $k_x = \pi - \delta k_x$. The Fermi arcs end around $\delta k_x = 0.6$ and the gap observed in the last panel is the standard nodal d-wave SC. (e)–(h) Theoretical results for the energy dependence of the spectral function $A(k, \omega)$ for cuts at fixed $k_x = \pi - \delta k_x$. The red dotted line is the noninteracting dispersion. We used the solution of Eq. (7) for the pseudogap amplitude and $Q_x = (0.2, 0)\pi$.

the x axis. Hot spots are points of the Fermi surface linked by (π, π) and are thus expected to be important due to the form of our interaction. Due to the finite wave vector of the pseudogap amplitude, the gap equation, Eq. (7), admits nonzero solution only in the ANR, when this modulation vector links two parts of the Fermi surface. The region close to the Brillouin zone diagonal will thus remain unperturbed by the transition at T^*. The electronic spectral function $A(\omega, k) = -\frac{1}{\pi}\mathrm{Im}[G(\omega + i\eta, k)]$ for $\omega = 0$ and $\eta \to 0^+$ shows that the ANR is gapped while the nodal region forms Fermi arcs [Fig. 1(c)]. These arcs terminate close to the hot spots.

We now look at the reconstructed band structure obtained from the zeros of $G^{-1}(k, \omega)$ in the ANR. From the form of $\tilde{G}(k, \omega)$, we can understand the dispersion as coming from an equal superposition of SC and CDW order in the ANR. We can thus construct the resulting band structure in the pseudogap as the hybridization of the three bands ξ_k, the normal state dispersion, $-\xi_k$ coming from the superconducting order, and ξ_{k+Q} coming from the modulating order. At the zone boundary ($k_x = \pi$), this results in two bands below the Fermi level shown in Fig. 1(d) with one of them presenting a back-bending (blue line) indicated by black arrows while the other one (yellow line) presents little dispersion around $k_y = 0$. In our mean-field description, this back-bending appears as a result of the hybridization between the hole band $-\xi_k$ (green dotted) and the shifted ξ_{k+Q} (blue dotted) band in Fig. 1(d). As such this back-bending will occur at $k_y = k_G > k_F$ as long as $\xi_{k+Q} < \xi_k$, which is satisfied for all $k_x > k_{\text{hot spot}}$. This means that this anomalous back-bending will persist below T_c in the ANR but we will recover a standard back-bending at $k_y = k_F$ in the nodal region as the above condition is not satisfied.

The spectral weight $A(k, \omega)$ for each band is obtained for different fixed values of $k_x = \pi - \delta k_x$ and compared to the experimental dispersion of Ref. [6] [Figs. 2(a)–2(d)]. As we get closer to the center of the Brillouin zone we can see that the energy of the maximum of the band gets closer to the Fermi level leading to the pseudogap closing "from below" [Figs. 2(e)–2(h)] as observed experimentally. Note that we obtain here a gap closing from below contrary to what was argued previously for a pure CDW scenario with a modulation along the y direction [7]. This is because we consider a modulation wave vector along the x direction. This same orientation for the modulation wave vector has been used recently to explain ARPES results in Bi2201 through the idea of a quantum disorder PDW [8] and other theoretical approaches such as a superposition of CDW and PDW order [9] or a RES [10].

Our previous description of the band structure in the pseudogap also shows a second band located at the bottom of the noninteracting band. Here we connect this band to the flatband observed experimentally below T_c [green dots in Figs. 2(a)–2(c)] and argue that finite lifetimes for the single-particle and pair excitations lead to this band not being observed above T_c. For this, we add three phenomenological damping rates Γ_0, Γ_1, and Γ_2 in our mean-field Green's function:

$$G^{-1}(i\omega, k) = i\omega - \xi_k - i\Gamma_0 - \sum_{Q=\pm Q_x, \pm Q_y} \frac{|\Psi_k|^2}{2} \tilde{G}(i\omega, k),$$
$$\tilde{G}(i\omega, k) = (i\omega - \xi_{k+Q} + i\Gamma_1)^{-1} + (i\omega + \xi_k + i\Gamma_2)^{-1}. \quad (8)$$

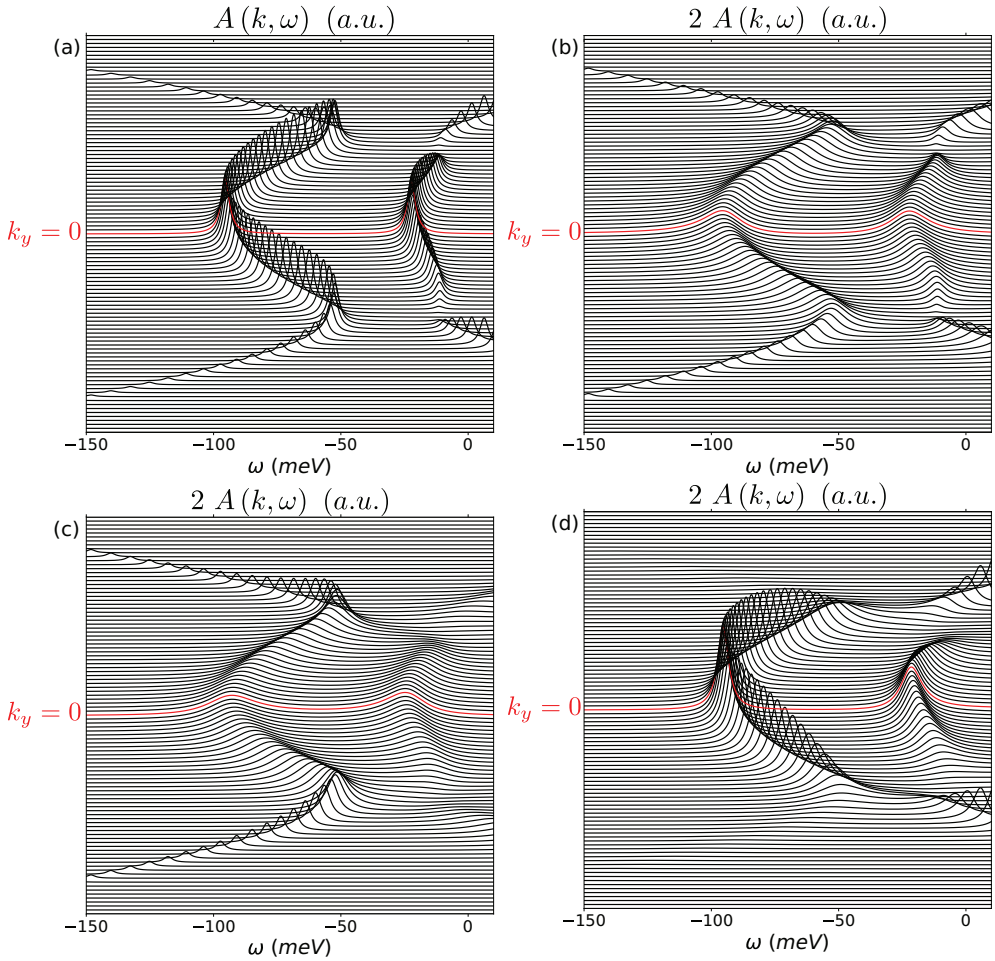

FIG. 3. Energy dependence of the spectral function at $k_x = \pi$ for different k_y between $-\pi/4$ and $\pi/4$; successive lines are shifted for clarity. (a) Without any lifetime $\Gamma_0 = \Gamma_1 = \Gamma_2 = 0$. We used a broadening $\eta = 0.002$ eV for numerical purposes. (b) Turning on a single-particle lifetime $\Gamma_0 = 0.02$ eV leads to both bands being broadened in a similar way. (c) In contrast, when we consider only a finite particle-hole lifetime $\Gamma_1 = 0.02$ eV we see that the dispersion close to $k_y = 0$ is more strongly affected than the dispersion at higher momenta. The flatband is also more strongly dampened than the main band. (d) The situation is reversed if we consider only a particle-particle lifetime $\Gamma_2 = 0.02$ eV. The parts of the bands close to $k_y = 0$ are less affected and still well defined. The flatband is more broadened but remains visible.

The two factors Γ_1 and Γ_2 represent the lifetime of particle-hole and particle-particle pairs, respectively [17–19]. These lifetimes capture the fluctuations in the pseudogap phase and are used in other approaches such as preformed pairs [20–23] or effect of Gaussian fluctuations [24]. They are expected to be nonzero above T_c but to vanish at the transition temperature when fluctuations are quenched. The first Γ_0 term is a single-particle lifetime which is always nonzero. The effect of each of these additional terms is depicted in Figs. 3(a)–3(d). Allowing a nonzero Γ_0 will broaden the two bands below the Fermi level in similar ways [Fig. 3(b)], in contrast to the pair lifetimes which have a very different effect on specific parts of the dispersion. Indeed, Fig. 3(c) shows that a nonzero Γ_1 will strongly suppress the flatband close to the Fermi level and also dampen the main band close to $k_y = 0$. Turning on the Γ_2 term will have the opposite effect as the band far from $k_y = 0$ gets dampened while the bottom of the flat- and main bands remain well defined. The experimental observation of the flatband only close or below T_c can then be attributed to the presence of a particle-hole pair lifetime in the pseudogap. Note also that due to disorder effects, which couple directly to charge order [25], this lifetime could remain nonzero below T_c and thus leads to this band remaining broad even in the superconducting state as observed experimentally. Moreover, this description provides good agreement with the experimental observation that the dispersion in the ANR does not change across the superconducting transition. In our case, the position of the main band does not change with temperature and only the spectral weights of the two bands get modified as the different lifetimes decrease.

Another feature of the temperature dependence measured experimentally for $T^* > T > T_c$ in the ANR is a significant decrease of the energy of the bottom of the band when the temperature is decreased while the maximum energy and the back-bending wave vector change only slightly as shown in Fig. 4(a). Here we describe this change in the band structure by adding a finite amplitude for the particle-hole order parameter $|\chi_k|$. We then have three different regions such that at $T > T^*$ we have free electrons: At $T \lesssim T^*$ where the pseudogap has a finite amplitude but the particle-hole gap is still 0 and at $T \gtrsim T_c$ where the particle-hole gap is finite. We then obtain the band dispersions shown in Fig. 4(b). Because

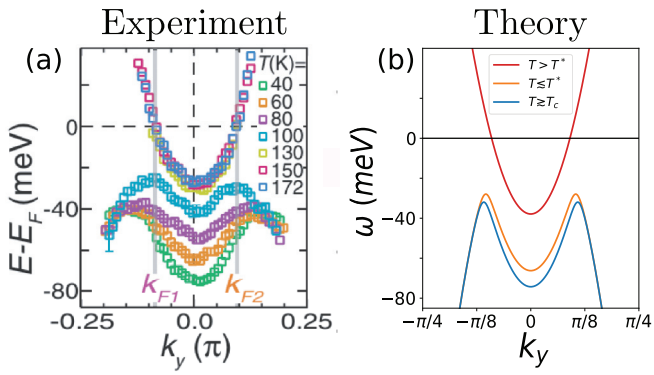

FIG. 4. Temperature evolution of the band at the zone edge in the pseudogap regime. (a) Experimental measurement for a range of temperature going from above $T^* \sim 132$ K to $T \gtrsim T_c \sim 38$ K [6]. (b) The red line indicates the noninteracting band above T^*. The orange line is the band after the opening of the pseudogap presenting a back-bending shifted from the original Fermi momentum k_F. When going down in temperature we add a finite mean-field amplitude for the CDW order and obtain the band dispersion represented in blue. The back-bending wave vector and the gap with respect to the Fermi level are mainly unchanged while the bottom of the band is strongly affected.

the bottom of the band is directly related to the hybridization with the band coming from the charge modulation, it is directly affected by the nonzero value of $|\chi_k|$. On the other hand, the back-bending momentum is determined mainly by the value of the modulation wave vector Q and the energy of the maximum comes from the hybridization between the superconducting band $-\xi_k$ and the shifted band ξ_{k+Q}, thus related to the value of $|\Psi_k|$. In contrast, a finite amplitude for the SC order parameter $|\Delta_k|$ would produce the opposite effect and change substantially the position of the maximum leaving the bottom of the band unchanged [15]. The fact that $|\chi_k|$ acquire a quasi-long-range component before the $|\Delta_k|$ is representative of the fact that CDW is observed experimentally at a temperature higher than the temperature for SC fluctuations T_c'. This long-range component of the CDW order has also been observed by Raman spectroscopy [26], x-ray [27–32], and NMR [33–36] measurements above T_c.

In conclusion, we showed here how the recently proposed idea of fractionalized PDW [3] can be used to construct a mean-field description of the pseudogap phase of cuprates. The main idea is that even if none of the CDW or SC orders develop a long-range component, the constraint introduced by the fractionalization affects the electronic Green's function. Using a microscopic model we derived a self-consistent equation for the pseudogap amplitude and showed that it has nonzero solutions in the antinodal region, which gives a gap in the ANR in the PG phase and leads to the formation of Fermi arcs. The band dispersion obtained in the antinodal region is in good agreement with the experimental ARPES measurement made on Bi2201. Specifically, we recover all the features observed in the pseudogap state. The superposition of particle-particle and particle-hole orders leads to an anomalous back-bending of the main band below the Fermi level, a gap closing from below and a flatband close to the bottom of the original electronic dispersion. We argue that this band is seen experimentally only below T_c because it is strongly affected by the finite pair lifetime in the pseudogap phase. Lastly, we discussed the change of the dispersion as the temperature is lowered from T^* to T_c by showing that a finite quasi-long-range component of the particle-hole order leads to the minimum of the band going down in energy while the energy and momentum of the maximum stay unchanged.

The competition between different orders is present in many other materials such as transition metal dichalcogenides [37], for example. We showed here that considering an entanglement between these competing orders has unique consequences beyond the standard competing scenarios. This idea could also be used to study other materials that exhibit pseudogap physics such as $CeRhIn_5$ [38] and $NbSe_2$ [39,40].

We thank S. Sarkar and A. Banerjee for valuable discussions. This work has received financial support from the ERC, under Grant agreement. No. AdG-694651-CHAMPAGNE.

[1] H. Alloul, T. Ohno, and P. Mendels, Phys. Rev. Lett. **63**, 1700 (1989).
[2] W. W. Warren, R. E. Walstedt, G. F. Brennert, R. J. Cava, R. Tycko, R. F. Bell, and G. Dabbagh, Phys. Rev. Lett. **62**, 1193 (1989).
[3] D. Chakraborty, M. Grandadam, M. H. Hamidian, J. C. S. Davis, Y. Sidis, and C. Pépin, Phys. Rev. B **100**, 224511 (2019).
[4] P. A. Lee, N. Nagaosa, and X.-G. Wen, Rev. Mod. Phys. **78**, 17 (2006).
[5] M. R. Norman and C. Pépin, Rep. Prog. Phys. **66**, 1547 (2003).
[6] R.-H. He, M. Hashimoto, H. Karapetyan, J. D. Koralek, J. P. Hinton, J. P. Testaud, V. Nathan, Y. Yoshida, H. Yao, K. Tanaka *et al.*, Science **331**, 1579 (2011).
[7] P. A. Lee, Phys. Rev. X **4**, 031017 (2014).
[8] Z. Dai, Y.-H. Zhang, T. Senthil, and P. A. Lee, Phys. Rev. B **97**, 174511 (2018).
[9] Y. Wang, D. F. Agterberg, and A. Chubukov, Phys. Rev. Lett. **114**, 197001 (2015).
[10] X. Montiel, T. Kloss, and C. Pépin, Europhys. Lett. **115**, 57001 (2016).
[11] G. Baskaran and P. W. Anderson, Phys. Rev. B **37**, 580 (1988).
[12] N. Nagaosa and P. A. Lee, Phys. Rev. Lett. **64**, 2450 (1990).
[13] P. A. Lee and N. Nagaosa, Phys. Rev. B **46**, 5621 (1992).
[14] M. Grandadam, D. Chakraborty, and C. Pépin, J. Superconductivity Novel Magnetism **33**, 2361 (2020).
[15] See Supplemental Material at http://link.aps.org/supplemental/10.1103/PhysRevB.102.121104 for details of the calculation and additional results on the separate roles of the CDW and SC orders.
[16] V. Hinkov, P. Bourges, Y. Pailhès, S. Sidis, A. Ivanov, C. D. Frost, T. G. Perring, C. T. Lin, D. P. Chen, and B. Keimer, Nat. Phys. **3**, 780 (2007).

[17] M. R. Norman, M. Randeria, H. Ding, and J. C. Campuzano, Phys. Rev. B **52**, 615 (1995).
[18] S. Banerjee, T. V. Ramakrishnan, and C. Dasgupta, Phys. Rev. B **84**, 144525 (2011).
[19] S. Banerjee, T. V. Ramakrishnan, and C. Dasgupta, Phys. Rev. B **83**, 024510 (2011).
[20] M. R. Norman, M. Randeria, H. Ding, and J. C. Campuzano, Phys. Rev. B **57**, R11093(R) (1998).
[21] C.-C. Chien, Y. He, Q. Chen, and K. Levin, Phys. Rev. B **79**, 214527 (2009).
[22] J. C. Campuzano, M. R. Norman, H. Ding, M. Randeria, T. Yokoya, T. Takeuchi, T. Takahashi, T. Mochiku, K. Kadowaki, P. Guptasarma, and D. G. Hinks, Nature (London) **392**, 157 (1998).
[23] J. C. Campuzano, H. Ding, M. R. Norman, and M. Randeira, Phys. Rev. B **53**, R14737(R) (1996).
[24] L. Benfatto, S. Caprara, and C. D. Castro, Eur. Phys. J. B **17**, 95 (2000).
[25] A. Del Maestro, B. Rosenow, and S. Sachdev, Phys. Rev. B **74**, 024520 (2006).
[26] B. Loret, N. Auvray, Y. Gallais, M. Cazayous, A. Forget, D. Colson, M.-H. Julien, I. Paul, M. Civelli, and A. Sacuto, Nat. Phys. **15**, 771 (2019).
[27] J. Chang, E. Blackburn, A. T. Holmes, N. B. Christensen, J. Larsen, J. Mesot, R. Liang, D. A. Bonn, W. N. Hardy, A. Watenphul, M. v. Zimmermann, E. M. Forgan, and S. M. Hayden, Nat. Phys. **8**, 871 (2012).
[28] S. Blanco-Canosa, A. Frano, T. Loew, Y. Lu, J. Porras, G. Ghiringhelli, M. Minola, C. Mazzoli, L. Braicovich, E. Schierle *et al.*, Phys. Rev. Lett. **110**, 187001 (2013).
[29] E. Blackburn, J. Chang, M. Hücker, A. T. Holmes, N. B. Christensen, R. Liang, D. A. Bonn, W. N. Hardy, U. Rütt, O. Gutowski *et al.*, Phys. Rev. Lett. **110**, 137004 (2013).
[30] G. Ghiringhelli, M. Le Tacon, M. Minola, S. Blanco-Canosa, C. Mazzoli, N. B. Brookes, G. M. De Luca, A. Frano, D. G. Hawthorn, F. He *et al.*, Science **337**, 821 (2012).
[31] S. Gerber, H. Jang, H. Nojiri, S. Matsuzawa, H. Yasumura, D. A. Bonn, R. Liang, W. N. Hardy, Z. Islam, A. Mehta *et al.*, Science **350**, 949 (2015).
[32] J. Chang, E. Blackburn, O. Ivashko, A. T. Holmes, N. B. Christensen, M. Hucker, R. Liang, D. A. Bonn, W. N. Hardy, U. Rutt *et al.*, Nat. Commun. **7**, 11494 (2016).
[33] T. Wu, H. Mayaffre, S. Krämer, M. Horvatic, C. Berthier, W. N. Hardy, R. Liang, D. A. Bonn, and M.-H. Julien, Nature (London) **477**, 191 (2011).
[34] T. Wu, H. Mayaffre, S. Krämer, M. Horvatić, C. Berthier, P. L. Kuhns, A. P. Reyes, R. Liang, W. N. Hardy, D. A. Bonn, and M.-H. Julien, Nat. Commun. **4**, 2113 (2013).
[35] T. Wu, H. Mayaffre, S. Krämer, M. Horvatić, C. Berthier, W. N. Hardy, R. Liang, D. A. Bonn, and M.-H. Julien, Nat. Commun. **6**, 6438 (2015).
[36] M.-H. Julien, Science **350**, 914 (2015).
[37] S. Koley, N. Mohanta, and A. Taraphder, Eur. Phys. J. B **93**, 77 (2020).
[38] S. Kawasaki, M. Yashima, T. Mito, Y. Kawasaki, G.-Q. Zheng, Y. Kitaoka, D. Aoki, Y. Haga, and Y. Ōnuki, J. Phys.: Condens. Matter **17**, S889 (2005).
[39] S. V. Borisenko, A. A. Kordyuk, V. B. Zabolotnyy, D. S. Inosov, D. Evtushinsky, B. Büchner, A. N. Yaresko, A. Varykhalov, R. Follath, W. Eberhardt *et al.*, Phys. Rev. Lett. **102**, 166402 (2009).
[40] U. Chatterjee, J. Zhao, M. Iavarone, R. D. Capua, J. P. Castellan, G. Karapetrov, C. D. Malliakas, M. G. Kanatzidis, H. Claus, J. P. C. Ruff *et al.*, Nat. Commun. **6**, 6313 (2015).